Production of Biodegradable Board using Rape Straw and Analysis of Mechanical Properties

Lili Huang,[a,b] Ping Xia,[b] Yamei Liu,[a] Yao Fu,[c] Yuanye Jiang,[c] Shengquan Liu,[a,*] and Xiulun Wang [b,d,*]

This study investigated the glueless preparation of biomass board using rape straw on a laboratory scale. The board-making process was broken down into four steps: soaking, refining, shape recovery, and hot-pressing. To observe the effect of pressure during the hot-press stage on the strength of the bio-board, five panels were manufactured at various pressures. Moreover, density functional theory (DFT) was used to explore how varying the pressure influenced the strength properties of the board. As pressure increased, the density of these five panels changed from 0.95 to 1.12 g/cm^3. The mechanical tests showed that the bending rupture strength of these panels changed from 43 to 53 MPa, while the tensile rupture strength changed from 27 to 33 MPa. The bending strength of these biomass boards performed well enough to qualify them as Type-35 board, and their density classified them as hardboard, according to the Japanese industrial standards (JIS). This study showed that board-making was feasible using rape straw. The experimental results and the density functional theory results were consistent, in that the mechanical properties of the panels improved with increasing pressure. The DFT method was shown to be useful in exploring the factors that influenced the strength properties of the biomass board on the microscopic scale.

Keywords: Rape straw; Board-making process; Mechanical property; Hydrogen bond; DFT method

*Contact information: a: College of Forestry and Gardening, Anhui Agricultural University, Hefei 230036, P. R. China; b: School of Engineering, Anhui Agricultural University, Hefei, 230036, P.R. China; c: Department of Chemistry, University of Science and Technology of China, Hefei 230026 , P.R. China; d: Faculty of Bioresources, Mie University, Tsu 5148507, Japan; * Corresponding authors: liusq@ahau.edu.cn; wang@bio.mie-u.ac.jp*

INTRODUCTION

Rape straw is an important economic crop in China, and oil can be produced from its fruit. According to the China rural statistical yearbook (DRSES 2013), in China, the total sown area of rape is approximately 7.43 million hectares, and the yield can reach 1.40 million tons, producing 4.02 million tons of rape straw every year. Burning or returning these straws to the field are the common methods of disposal, but they may create unfavorable impacts on the ecosystem.

To utilize this kind of agricultural residue productively, much research has been conducted concerning the use of rape straw to produce bioethanol (Arvaniti *et al.* 2012; Ji *et al.* 2014). Rape straw consists primarily of cellulose, hemicellulose, lignin, and ash (Alexander *et al.* 1987). Because rape straw consists predominantly of cellulose, like wood, it can be used as an alternative to wood as a raw material to produce boards.

At present, China is one of the largest consumers of timber and wood-based panels in the world. China's forest area per capita (FAPC) is only 0.132 hectares, and this figure is decreasing with the growth of the population. An imbalance between the domestic timber production from natural forests and the consumption in the panel industry is creating an ever-increasing gap. China remedies this gap by importing timber or by producing non-wood-based composites. Worldwide, the situation is very similar. There appear to be a plethora of adhesive-bonded panels based on crop straws that have been studied in foreign (Ye *et al.* 2007; Yousefi 2009) and domestic (Pan *et al.* 2009) research institutes. However, the carcinogenic or toxic emissions released during the manufacturing and use of adhesive-bonded panels are a serious problem (Hashim *et al.* 2009) that has driven the board market to call for composite panels without any synthetic adhesives.

Oil palm biomass has been used at the lab scale to manufacture particleboard panels without using any adhesives (Rokiah and Nadhari 2012). The results showed that this kind of binderless board can exhibit properties that meet the requirements stated in the Japanese industrial standard (JIS) to be classified as hardboard (HB) (JIS - A 5908 2003). Wheat straw was used as a raw material for the production of fiberboard in a previous study, in which adhesive bonding between fibers was initiated by adding hydrogen peroxide (Halvarsson *et al.* 2009). Increasing the concentration of hydrogen peroxide improved the mechanical properties of the fiberboard. A gluing method was invented for fiberboard that utilized laccase-activated tannin and wood fibers (Widsten *et al.* 2009), and the fiberboard prepared with laccase and the reactive tannin had superior mechanical properties. A dry-formed HB with a soybean-based adhesive was researched by Ye *et al.* (2005), and the soybean-based adhesive resulted in much better mechanical properties and water resistance than urea-formaldehyde resin.

The wet process is a method using water as the fiber-distributing medium during mat forming that has been used to produce binderless board for decades (Mobarak *et al.* 1982; Widsten and Kandelbauer 2014). The bonding mechanism that takes place during the HB manufacturing process has been studied using several methods (Suchsland *et al.* 1985; Back *et al.* 1987). The results concluded that inter-fiber bonding is very critical for the strength properties of the board, and most of the inter-fiber bonding is due to secondary bonds. The most dominant of these secondary bonds was found to be the hydrogen bonds between adjacent cellulose chains and their numerous hydroxyl groups.

Density functional theory (DFT) has been used to calculate Gibbs free energy changes. The thermodynamic energy change of cellulose pyrolysis through homolytic bond cleavage was studied with the aid of DFT using cellulose dimers as a model compound (Jiang *et al.* 2013). Gibbs free energy changes during the combination processes of a complex imply stability of this complex. Thus, the DFT method can be used to explore the factors that influence the strength properties of the board on a microscopic scale.

The goal of this paper was to prepare a biodegradable fiberboard from rape straw without adding any binder in the board-making procedure. To explore the relationship between the forming pressure and the properties of the fiberboard, various pressure conditions were used during the manufacturing process. The DFT method was also used to calculate the Gibbs free energy changes of the hydrogen bonds between adjacent cellulose chains, those between adjacent hemicelluloses chains, and those between a cellulose chain and a hemicellulose chain.

EXPERIMENTAL

Materials

This study utilized rape straw collected in the Anhui Province of China in 2014 as the raw material. After letting the straw air-dry naturally, the shells were cut and stems were selected for board-making. These stems were cut into 2-cm sections using a straw pulverizer (9DF360, Huaxiang, China).

Characterization of Raw Material

Fiber morphology and chemical composition analysis

The chemical composition of the rape straw was analyzed based on Chinese National Standards (GB/T 2677.8 1994, GB/T 2677.9 1994, GB/T 2677.10 1995, GB/T 742 2008). The rape straw fiber was segregated using a 1:1 mixture of glacial acetic acid and hydrogen peroxide. In total, 1,000 specimens of segregated fibers were observed through an optical microscope (E200, Nikon, Japan) at 100× magnification to analyze the fiber morphology.

TG and XRD characterization

The crystallinity of the rape straw was determined using an X-ray diffractometer (XD-3, Puxi, China), operating under Cu-Kα radiation (λ = 0.1540563 nm), with a scan rate of 1 °/min, an accelerating voltage of 36 kV, and a diffraction angle (2θ) ranging from 5° to 40°.

The weight loss rate of the raw material was analyzed using a thermogravimetric analyzer (TGA-209, Netzsch, Germany). Ten milligrams of rape straw powder was placed into the alumina crucible of the TGA-209 and heated at a rate of 10 °C/min from 40 to 700 °C.

Manufacturing Biomass Boards

Biomass boards were prepared through the wet process. First, the stem sections were pulverized with a grinding machine (MK-K48P, Panasonic, Japan) to fully expose the hydroxyl groups. The ground sections were immersed in water at room temperature (20 °C) for 72 h. The soaking process softened and swelled the fibers to reduce the probability of fiber cutting. After swelling, the fibers were passed through a high-speed refiner (SPM380-WF, Jinridong, China), which separated the fibers evenly with a high yield. This process produced microfibers with a larger specific surface area, allowing the fibers to interweave more easily. However, most of the fibers leaving the refiner were deformed and crimped (Fig. 1a), so the shape recovery process was used to allow them to recover their shape (*i.e.* removal of latency or curl). The pulp was heated to 90 °C, and the temperature was maintained for 30 min, after which the fibers were fully extended (Fig. 1b). This process is helpful for board-making because it increases the contact area between fibers. Next, the pulp was hot-pressed; the pulp was poured into a compression mold under the conditions shown in Table 1. The compression mold was stainless steel, designed to form a product that was 100 mm × 100 mm × 25 mm (Fig. 2a). An important auxiliary tool was a copper block (Fig. 2b), the same size as the mold cavity. It was used to extrude excess water from the die. Other auxiliary tools were an aluminum plate (Fig. 2c) and two metal mesh screens (Fig. 2d), all of the same size: 100 mm × 100 mm. To filter and evaporate the water, there were many 2-mm-diameter holes spaced at an interval of 7 mm × 7 mm in the bottom of the mold and the auxiliary tools. Water

between the fibers was squeezed, and the fibers were interwoven during the hot-pressing stage. Five panels (A, B, C, D, and E) were produced.
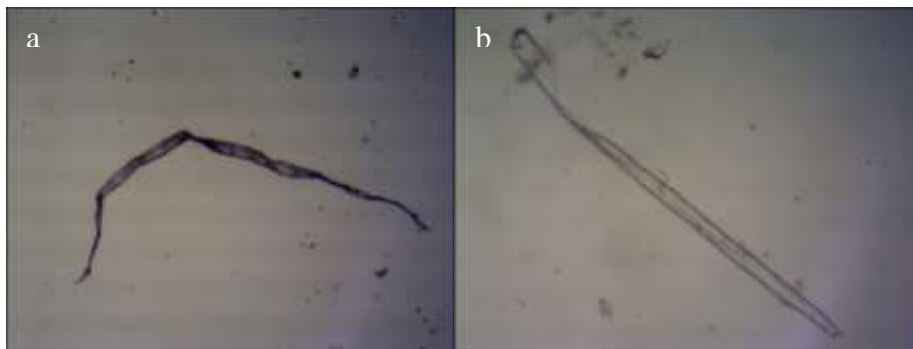

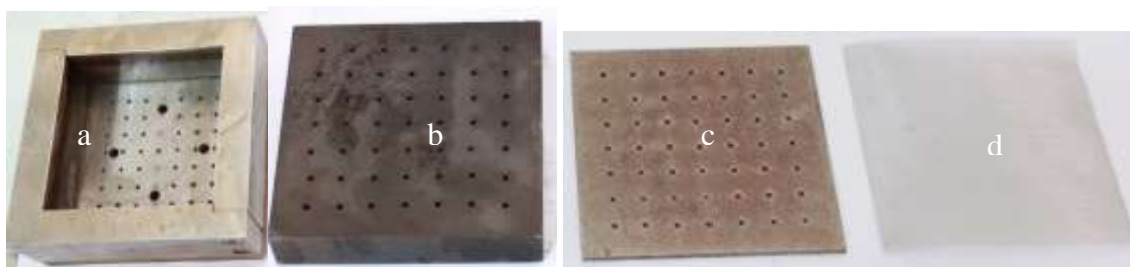**Fig. 1.** Fiber shape (a) before and (b) after the shape recovery process (100× magnification)

Fig. 2. Hot-press tools: (a) compression mold; (b) copper block; (c) aluminum plate; (d) metal mesh screen.

Table 1. Hot-Pressing Conditions

Panel	Temperature (°C)	Time (h)	Pressure (MPa)
A	110	2	2
B	110	2	3.5
C	110	2	5
D	110	2	6.5
E	110	2	8

Mechanical Testing

The bending strength and tensile strength are important mechanical characteristics for boards, and the biomass board samples produced were tested using a universal material machine (ETM103A, Wance, China). The dimensions of the specimens used for the bending and tensile tests are shown in Fig. 3.
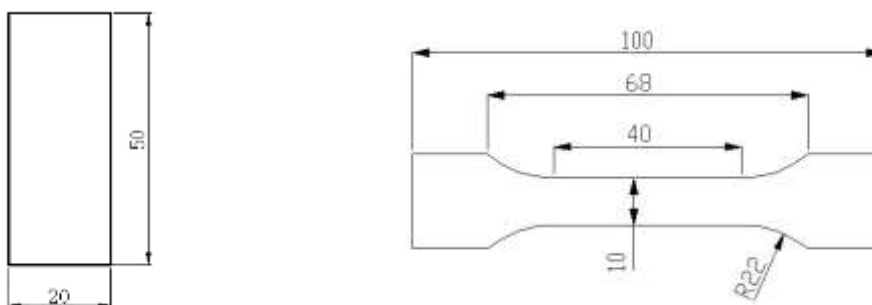

Fig. 3. Size of the test specimens (mm): left: bending test; right: tensile test

The experimental methods and standards used are shown in Table 2.

Table 2. Experimental Methods and Standards

Mechanical Characteristic	Test Method	Standard
Bending Strength	Three-Point Bending Test	JIS A 5905:2003 (JIS - A 5905 2003)
Tensile Strength	Tensile Test	JIS A 5905:2003 (JIS - A 5905 2003)

The bending strength was calculated according to Eq. 1,

$$\sigma_b = \frac{3PL_s}{2ba^2} \qquad (1)$$

where σ_b is bending strength, P is the applied load, L_S is the span of the supported points, b is the thickness of the specimen, and a is the width of the specimen. Equation 2 gives the corresponding expression for tensile strength,

$$\sigma = \frac{P}{A} \qquad (2)$$

where P is the applied load and A is the area of the specimen.

Density Functional Theory (DFT) Method

DFT study was performed by using the Gaussian 09 software package (Frisch *et al.* 2013) at the M06 level of theory (Zhao and Truhlar 2008). The "ultrafine" grid was assigned for all calculations to avoid possible integration grid errors (Gräfenstein *et al.* 2007). Geometry optimizations were performed in the gas phase with the basis set 6-31G (d) for all atoms. The typical chemical structure of hemicellulose of gramineous plants is xylopyranose (Schadel *et al.* 2010).

In this work glucose and xylopyranose were used as the models to simulate cellulose and hemicellulose, respectively. The geometry optimizations of glucose and xylopyranose were performed firstly; then, the optimized glucose and xylopyranose were put together in different orientations to form glucose-glucose, xylopyranose-xylopyranose, and glucose-xylopyranose complexes through hydrogen bonding. The structures of these complexes were further optimized, without structural constraints, to reach their energy minima.

At the same level of theory, based on the optimized structures, frequency analysis was performed to verify the stationary points as minima and to obtain Gibbs free energy corrections. To obtain a more accurate electronic energy, a larger basis set of 6-311++G(d,p) was assigned to all atoms to calculate the single-point energy based on the optimized structures.

Finally, the Gibbs free energies of glucose, xylopyranose, and the complexes were obtained by adding their corresponding Gibbs free energy corrections from the frequency analysis to their single-point energies. The Gibbs free energies of the complexes minus those of the two monomers under different pressures to calculate the Gibbs free energy changes of the corresponding combination processes. To compare the results with the experimental conditions, simulated conditions of pressure were specified at 2 MPa, 3.5 MPa, 5 MPa, 6.5 MPa, 8 MPa, and 9.5 MPa atmospheric pressure at a temperature of 383 K (110 °C).

RESULTS AND DISCUSSION

The chemical composition of rape straw is summarized in Table 3 and compared to that of rice straw. Based on this table, the proportion of ash in the rape straw was 4.62%, which was dramatically lower than in the rice straw, and the proportion of α-cellulose in the rape straw was 38.90%, slightly higher than in the rice straw. According to this comparison, the rape straw was more suitable for making fiberboard.

Table 3. Chemical Composition of Rape Straw Compared to Rice Straw

Chemical Component	Proportion in Rape Straw (%)	Proportion in Rice Straw (%)
α-Cellulose	38.90±1.34	34.61±0.98
Pentosan	17.98±0.75	17.45±1.24
Lignin	19.28±1.48	15.89±1.37
Ash	4.62±0.31	13.46±0.53

The fiber length distribution of rape straw is shown in Fig. 4, and the fiber morphology is summarized in Table 4. The results showed that 44% of the fibers were less than 1 mm long, 26% ranged from 1 to 1.5 mm, 19% spanned 1.5 to 2 mm, 7% varied between 2 and 3 mm, and the rest were longer than 3 mm. The average fiber length was 1.30 mm, the average width was 27.4 μm, and the length-to-width ratio was 47.3.
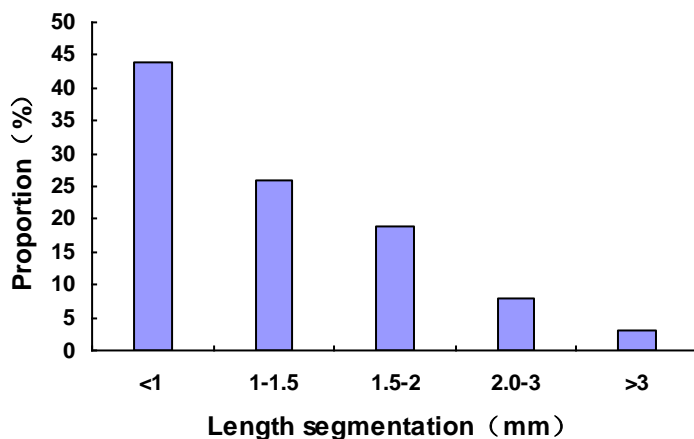

Fig. 4. Fiber length distribution of the rape straw

Table 4. Fiber Morphology of Rape Straw

Fiber Length (mm)			Fiber Width (μm)			Ratio Of Length to Width
Minima	Maxima	Average	Minima	Maxima	Average	
0.315	4.41	1.30±0.31	10.8	39.1	27.4±4.43	47.3

TG and XRD Characterization of Raw Material

Figures 5 and 6 show the TG and XRD characterizations of rape straw, respectively. Figure 5 demonstrates that at temperatures below 200 °C, the weight loss rate of the raw material was less than 95%. From 200 to 400 °C, the weight loss rate of

bioresources.com

the rape straw decreased from 95% to 30%. The relative crystallinity of the rape straw was calculated using diffraction intensities deviation method (Segal *et al.* 1959), shown as Eq. 3,

$$C_{rl} = \frac{I_{002} - I_{am}}{I_{002}} \times 100\%$$

(3)

where C_{rl} is the relative crystallinity, I_{002} is the amplitude of the (002) diffraction peak (typically for $2\theta \approx 22°$) and I_{am} is the intensity at $2\theta = 18°$. In Fig. 6, the value of I_{002} was 2845 and I_{am} was 1170, so the relative crystallinity was determined to be 58.87%.
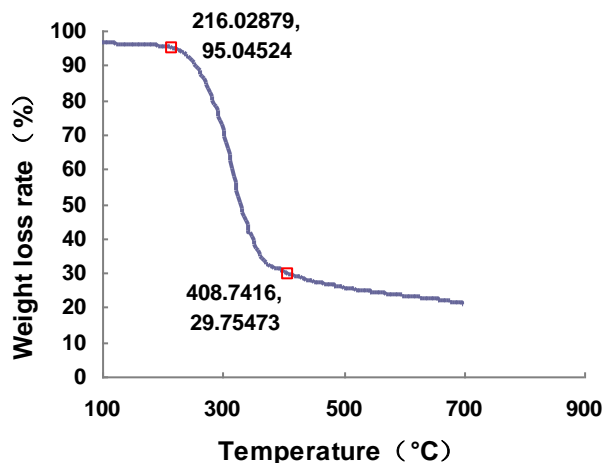
Fig. 5. TG characterization
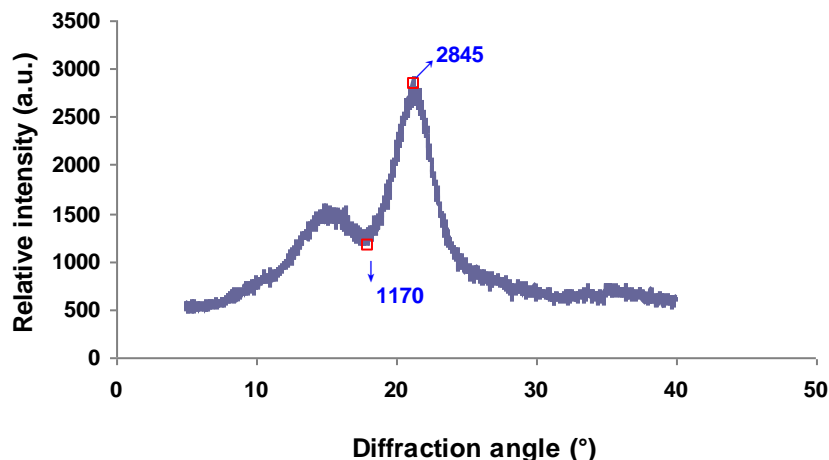
Fig. 6. XRD characterization

Density and Moisture Content of the Panels

The dimensions of the manufactured boards were 100 mm × 100 mm, while the thickness varied slightly (1.5 to 2 mm). The densities of the panels produced under various forming pressures are shown in Fig. 7. When the pressure increased from 2 to 8 MPa, the density increased from 0.95 to 1.12 g/cm³. The densities of these bio-boards exceeded 0.8 g/cm³, qualifying them as hardboards based on the JIS (JIS - A 5905 2003). Figure 8 displays the moisture content of the boards produced under various forming pressures. The moisture content fluctuated from 6.67% to 9.62% with no relation to pressure.
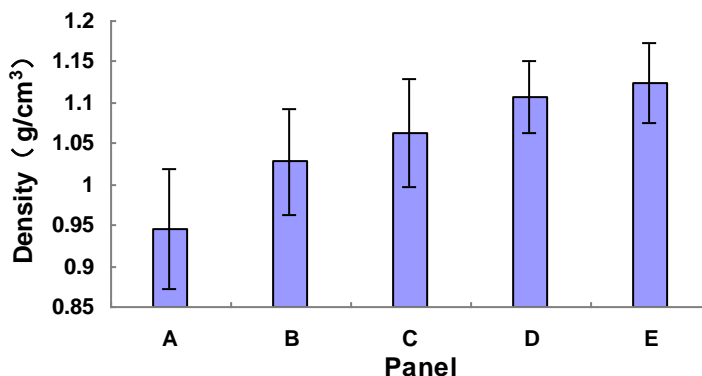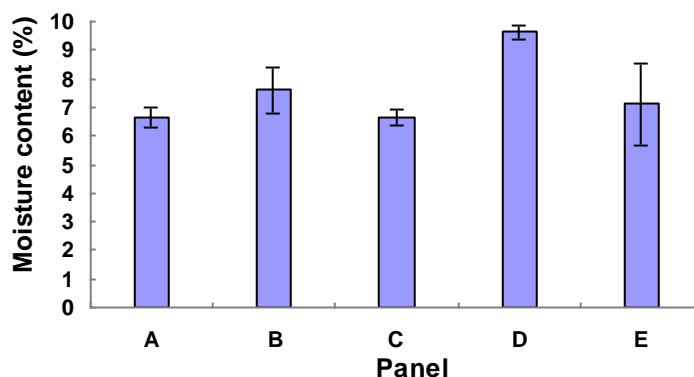
Fig. 7. Densities of the panels

Fig. 8. Moisture content of the panels

Mechanical Properties

Figure 9 exhibits the bending stress-strain curves of specimens cut from sample D, which were coded Db1, Db2, Db3, and Db4. During the initial stage, bending stress increased from 0 to 10 MPa. The second stage was the elastic stage, where bending stress grew from 10 to 35 MPa. The next stage was the elastic-plastic stage, during which the bending stress dropped swiftly to zero after it had reached the highest point for each specimen. For these four specimens, the stress-strain curves did not coincide entirely because the sample was not completely homogeneous.

Figure 10 shows the tensile stress-strain curves of specimens cut from sample D, which were termed Dt1, Dt2, and Dt3. These specimens showed a linear relationship between stress and strain before rupture occurred. The rupture happened at the end of the elastic stage, where the stress suddenly changed from the maximum to zero. For these three specimens, once again the stress-strain curves did not coincide entirely because this sample was also not homogeneous.

For the various panels, the bending rupture strength is shown in Fig. 11, and the tensile rupture strength is shown in Fig. 12. As forming pressure increased, the bending rupture stress of the panels increased from 43 to 53 MPa. The maximum rupture stress occurred in sample D, which was manufactured at a forming pressure of 6.5 MPa. The tensile rupture stress of the panels increased with pressure from 27 to 33 MPa; the maximum rupture stress also occurred in sample D. Compared to panel D, the bending rupture stress of panel E was approximately 1 MPa less, and the tensile rupture stress was approximately 1.2 MPa less.
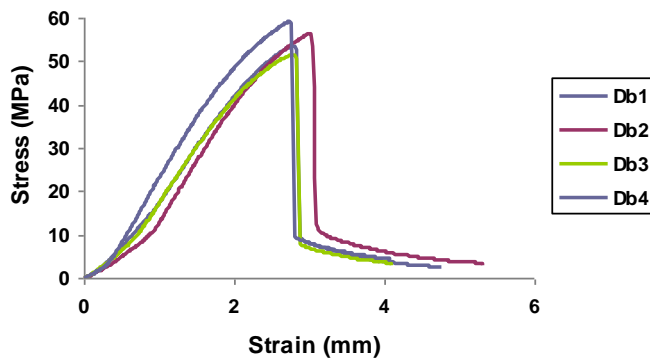
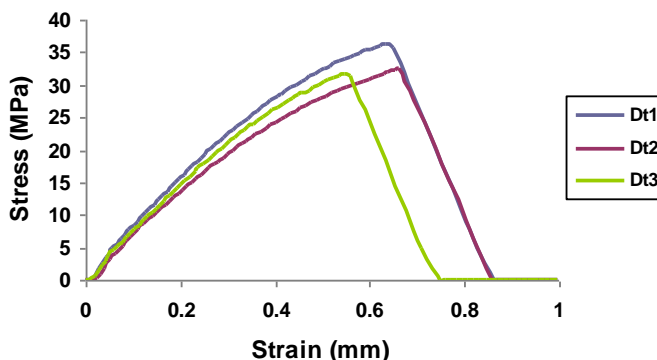**Fig. 9.** Bending stress-strain curves of specimens Db1, Db2, Db3, and Db4

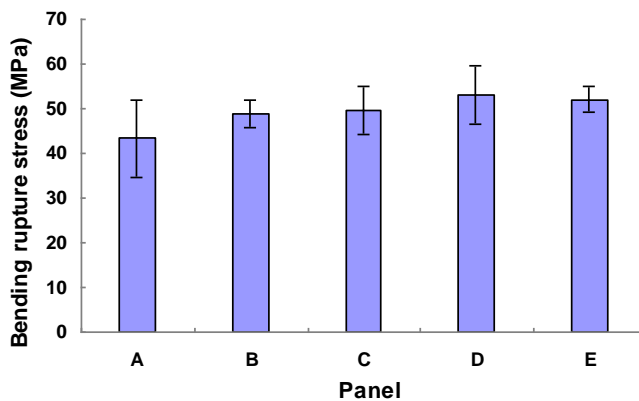**Fig. 10.** Tensile stress-strain curves of specimens Dt1, Dt2, and Dt3

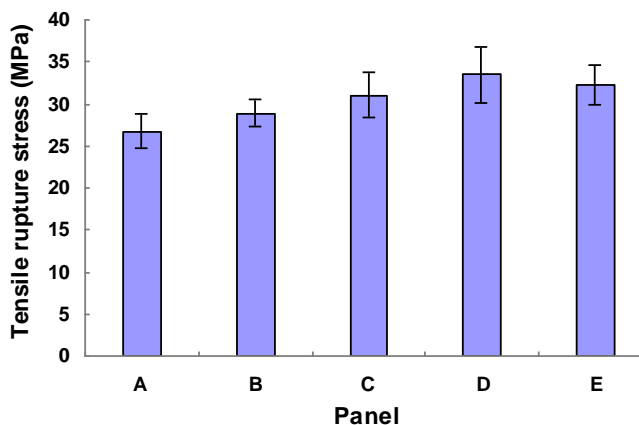**Fig. 11.** Bending rupture strength of the panels

Fig. 12. Tensile rupture strength of the panels

DFT Simulation of the Interaction of Cellulose and Hemicellulose

3D structures of the cellulose and hemicellulose models are displayed in Fig. 13. Glucose and xylopyranose can form glucose-glucose, xylopyranose-xylopyranose, and glucose-xylopyranose complexes through hydrogen bonding. The Gibbs free energy changes of these combination processes under different pressure at 110 °C were calculated (Fig. 14). Figure 14a shows how the complex could form by the interactions between the hydroxyl groups at the C4 and C6 sites of one glucose and those at the C1 and C2 sites of the other glucose. Figure 14b shows how the complex could form by the interactions between the hydroxyl groups at the C3 and C4 sites of one glucose and those at the C4 and C6 sites of the other glucose. Figure 14c shows how the complex could form by the interactions between the hydroxyl groups at the C3 site of one xylopyranose and the one at the C4 site of the other xylopyranose. Figure 14d shows how the complex could form by the interactions between the hydroxyl groups at the C3 site of one xylopyranose and those at the C2 and C4 sites of the other xylopyranose. Figure 14e shows how the complex could form by the interactions between the hydroxyl groups at the C4 site of glucose and the one at the C3 site of xylopyranose. Figure 14f shows how the complex could form by the interactions between the hydroxyl groups at the C2 and C3 sites of glucose and those at the C1 and C2 sites of xylopyranose. The O-H bond lengths of the hydrogen bonds in the different complexes varied between 1.820 and 2.065 Å after geometry optimizations. It was found that increasing the pressure could lead to lower Gibbs free energy changes for all of the combination processes considered, meaning that increasing pressure promotes the combination of hydroxyl-group-bearing materials like cellulose and hemicellulose.
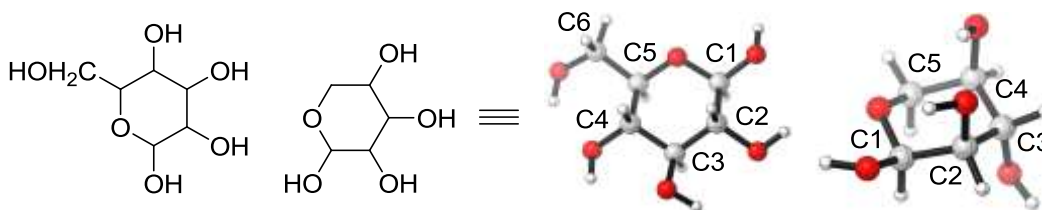

Fig. 13. Cellulose dimer model compound (red spheres denote oxygen, gray spheres denote carbon, and small white spheres denote hydrogen atoms)

Discussion

Binderless boards made from oil palm have a bending rupture strength of 10.9 MPa (Rokiah and Nadhari 2012). Binderless boards made from kenaf core showed a stronger performance, with a bending rupture strength of 36.1 MPa (Okuda and Sato 2004). The bending rupture strength of biomass boards made from rape straw was the highest among these three binderless boards, at 43 to 53 MPa, depending on the forming pressure. As a general summary, the results showed that it was possible to produce biodegradable biomass boards using rape straw.

This kind of biomass board could be used as packing boxes because of its strength properties (bending rupture strength exceeds 40 MPa and tensile rupture strength exceeds 20 MPa). The residue of the board could be reused for animal fodder because the board was produced without any additive or glue. Such board could also be processed into containers for seeding because of its biodegradability.
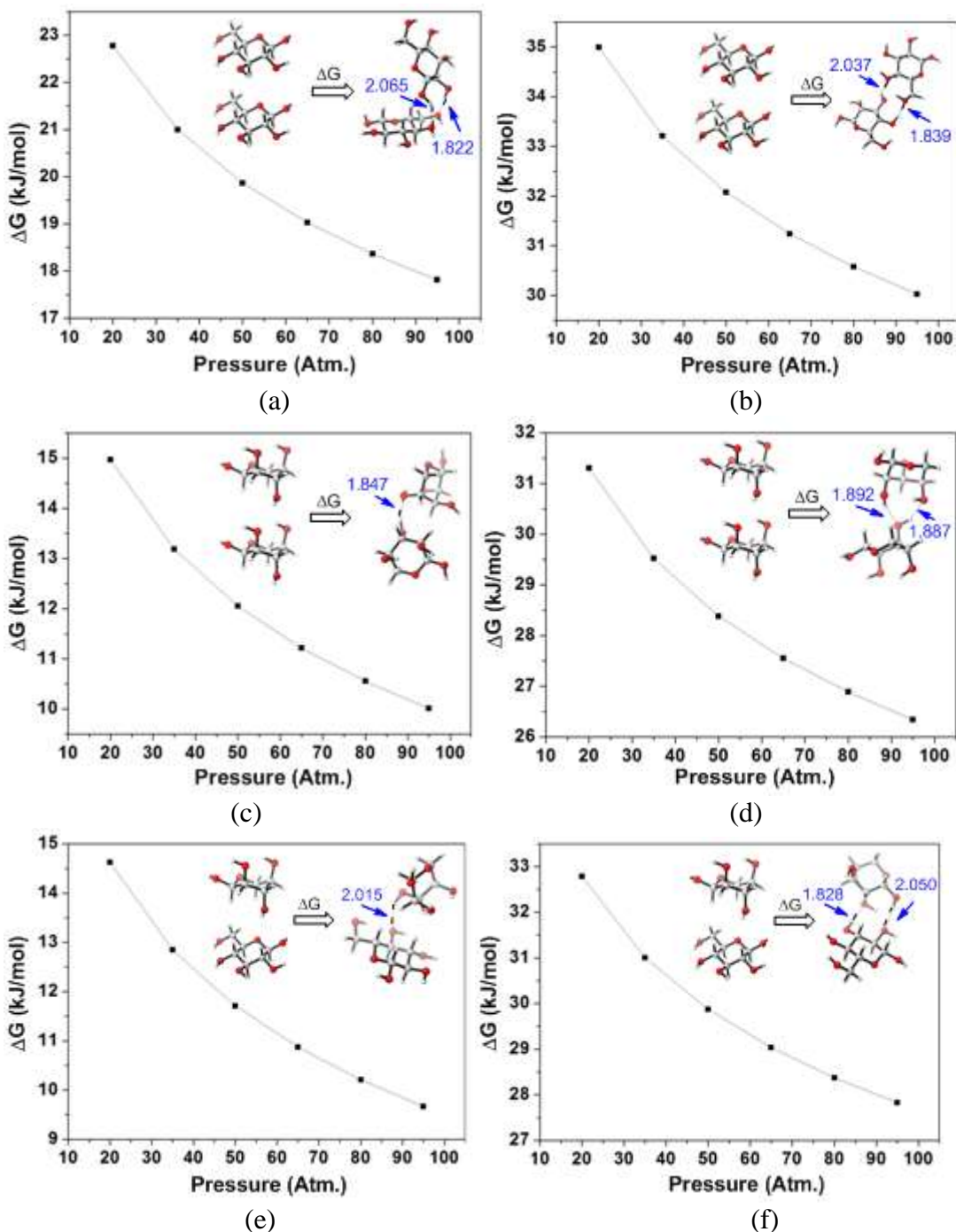
(a)

(b)

(c)

(d)

(e)

(f)

Fig. 14. Gibbs free energy changes resulting from the combination of two cellulose monomers under different pressures, and the 3D structures of geometry-optimized glucoses and their complexes

As the hot-press pressure increased to 6.5 MPa, the rupture stress of the biomass board also increased, dropping slightly at a pressure of 8 MPa. The pressure was likely so high that it caused some defects in the board. The DFT results indicated that high pressure promoted the combination of cellulose and hemicellulose. It follows that better mechanical properties can be expected following high pressure treatment.

bioresources.com

The results obtained from the DFT method were in accordance with the results from the mechanical testing, indicating that hydrogen bonds are critical to the strength properties of biomass board (Suchsland *et al.* 1985; Back *et al.* 1987), and high pressure is beneficial for board-making.

CONCLUSIONS

1. Biomass boards were successfully manufactured through a wet process, without any resin, using rape straw. The biomass boards performed well enough in bending strength to qualify as Type-35 board, and their densities met the criteria for HB. Based on JIS (JIS - A 5905 2003), Type-35 board is classified by its bending strength and the minimum requirements for the bending strength is 35 MPa.

2. The DFT method was useful for exploring the factors that influence the strength properties of the board on a microscopic scale.

REFERENCES CITED

Arvaniti, E., Bjerre, A. B., and Schmidt, J. E. (2012). "Wet oxidation pretreatment of rape straw for ethanol production," *Biomass Bioenerg.* 39(4), 94-105. DOI: 10.1016/j.biombioe.2011.12.040

Alexander, B. W., Gordon, A. H., Lomax, J. A., and Chesson, A. (1987). "Composition and rumen degradability of straw from 3 varieties of oilseed rape before and after alkali, hydrothermal and oxidative treatment," *J. Sci. Food Agric.* 41(1), 1-15. DOI: 10.1002/jsfa.2740410102

Back, E. L. (1987). "The bonding mechanism in hardboard manufacture review report," *Holzforschung* 41(4), 247-258. DOI: 10.1515/hfsg.1987.41.4.247

DRSES (Department of rural socio-economic survey), NBSC (National Bureau of Statistics of China) (2013). "China Rural Statistical Yearbook," *China Statistics Press*, Beijing, China.

Frisch, M. J., Trucks, G. W., Schlegel, H. B., Scuseria, G. E., Robb, M. A., Cheeseman, J. R., Scalmani, G., Barone, V., Mennucci, B., Petersson, G. A., *et al.* (2013). *Gaussian 09, Revision D.01*, Gaussian, Inc., Wallingford, CT.

Gräfenstein, J., Izotov, D., and Cremer, D. (2007). "Avoiding singularity problems associated with meta-GGA (generalized gradient approximation) exchange and correlation functionals containing the kinetic energy density," *J. Chem. Phys.* 127(21). DOI: 10.1063/1.2800011

GB/T 2677.8 (1994). "Fibrous raw material - Determination of acid insoluble lignin," National Standardization Technical Committee, Beijing, China.

GB/T 2677.10 (1995). "Fibrous raw materials - Determination of holocellulose," National Standardization Technical Committee, Beijing, China.

GB/T 742 (2008). "Fibrous raw material, pulp, paper and board - Determination of ash," National Standardization Technical Committee, Beijing, China.

GB/T 2677.9 (1994). "Fibrous raw materials - Determination of pentosan," National Standardization Technical Committee, Beijing, China.

Halvarsson, S., Edlund, H., and Norgen, M. (2009). "Manufacture of non-resin wheat straw fibreboards," *Ind. Crop. Prod.* 29(2-3), 437-445. DOI:10.1016/j.indcrop.2008.08.007

Hashim, R., Hamid, S. H. A., Sulaiman, O., Ismail, N., Ibrahim, M. H., Jais, H., and Ujang, S. (2009). "Extractable formaldehyde from waste medium density fibreboard," *J. Trop. Forest Sci.* 21(1), 25-33.

Ji, W., Shen, Z., and Wen, Y. (2014). "A continuous hydrothermal saccharification approach of rape straw using dilute sulfuric acid," *BioEnergy Res.* 7(4), 1392-1401. DOI: 10.1007/s12155-014-9468-y

JIS - A 5908 (2003). "Particleboards," Japanese Standard Association, Tokyo, Japan.

JIS - A 5905 (2003). "Fiberboards," Japanese Standard Association, Tokyo, Japan.

Jiang, Y., Yu, H., and Fu, Y. (2013). "Theoretical study on thermodynamic properties of pyrolysis of cellulose dimer model compound," *Acta Chim. Sinica* 71(12), 1611-1619. DOI: 10.6023/A13070765

Mobarak, F., Fahmy, Y. and Augustin H. (1982). "Binderless lignocellulose composite from bagasse and mechanism of selfbonding," *Holzforschung* 36(3), 131-135.

Okuda, N., and Sato, M. (2004). "Manufacture and mechanical properties of binderless boards from kenaf core," *J. Wood Sci.* 50(1), 53-61. DOI: 10.1007/s10086-003-0528-8

Pan, M. Z., Zhou, D. G., Deng, J., and Zhang, S. Y. (2009). "Preparation and properties of wheat straw fiber-polypropylene composites. I. Investigation of surface treatments on the wheat straw fiber," *J. Polym. Sci.*114(5), 3049-3056. DOI: 10.1002/app.30325

Rokiah, H., and Nadhari, W. N. A. W. (2012). "Properties of binderless particleboard panels manufactured from oil palm biomass," *BioResources* 7(1), 1352-1365. DOI: 10.15376/biores.7.1.1352-1365

Schadel, C., Bochl, A., Richter, A., and Hoch, G. (2010). "Quantification and monosaccharide composition of hemicelluloses from different plant functional types," *Plant Physiol. Bioch.* 48, 1-8. DOI: 10.1016/j.plaphy.2009.09.008

Suchsland, O., Woodson, G. E., and McMillan, C. W. (1985). "Binderless fiberboard from two different types of fiber furnishes," *Forest Prod. J.* 35(2), 63-68.

Segal, L., Creely, J., Martin, A., and Conrad, C. (1959). "An empirical method for estimating the degree of crystallinity of native cellulose using the X-ray diffractometer," *Text. Res. J.* 29(10), 786-794. DOI: 10.1177/004051755902901003

Widsten, P., and Kandelbauer, A. (2014)."Industrial scale evaluation of cationic tannin as a binder for hardboard," *J. Adhes. Sci. Technol.* 28(13), 1256-1263. DOI: 10.1080/01694243.2014.896068

Widsten, P., Hummer, A., Heathcote, C., and Kandelbauer, A. (2009). "A preliminary study of green production of fiberboard bonded with tannin and laccase in a wet process," *Holzforschung* 63(5), 545-550. DOI: 10.1515/HF.2009.090

Ye, X., Julson, J., Kuo, M., and Myers, D. (2005)."Biocomposite hardboard from renewable biomass bonded with soybean-based adhesive," *Trans. ASAE* 48(4), 1629-1635.

Ye, X. P., Julson, J., Kuo, M., Womac, A., and Myers, D. (2007). "Properties of medium density fiberboards made from renewable biomass," *Bioresour. Technol.* 98(5),1077-1084. DOI: 10.1016/j.biortech.2006.04.022

Yousefi, H. (2009). "Canola straw as a bio-waste resource for medium density fiberboard (MDF) manufacture," *Waste Manage.* 29(10), 2644-2648. DOI: 10.1016/j.wasman.2009.06.018

Zhao, Y., and Truhlar, D. G. (2008). "The M06 suite of density functionals for main group thermochemistry, thermochemical kinetics, noncovalent interactions, excited states, and transition elements: Two new functionals and systematic testing of four M06-class functionals and 12 other functionals," *Theor. Chem. Acc.* 120(1-3), 215-241. DOI: 10.1007/s00214-007-0310-x.